Self-Assembly of Quantum-Dot Molecules: Heterogeneous Nucleation of SiGe Islands on Si(100)

X. Deng and M. Krishnamurthy*

Department of Metallurgical and Materials Engineering, Michigan Technological University, Houghton, Michigan 49931

(Received 22 April 1998)

We report on the formation of clusters of self-assembled quantum dots (termed quantum-dot molecules). Each cluster, typically consisting of four closely spaced SiGe islands, is formed by preferential nucleation around the edges of square pits. Uniform-sized pits are directly formed by controlled deposition of Si and C on the initial Si(100) surface, followed by the growth of a thin Si buffer layer. Formation of {105} pit walls as precursors to island formation and elastic relaxation effects near the pits appear to influence island nucleation. Quantum-dot molecules may have potential applications in nanoelectronic devices and may exhibit novel electronic and optical properties. [S0031-9007(98)06938-5]

PACS numbers: 68.55.Jk

Quantum dots are zero-dimensional structures that offer a pathway for tuning the physical, electronic, and optical properties of materials by controlling their size. These quantum dots (also referred to as "artificial atoms") have been fabricated using a variety of techniques, from solute precipitation [1] to epitaxial growth [2]. In particular, islands formed during epitaxial growth [3–5] (or annealing [6]) of lattice-mismatched semiconductors (e.g., Ge/Si, InAs/GaAs) have been observed to have a very uniform size [7] and have been used for the direct fabrication of quantum dots [2]. For optical applications, an ensemble of uniform sized, but randomly distributed dots may be adequate; however, for most electronics applications, a more controlled spatial arrangement would seem to be required. One such application is the quantum cellular automata (QCA) [8], a transistorless approach to computation, that offers an alternative to the field-effect transistor (FET)-based paradigm [9]. The simplest QCA cell consists of four coupled (by tunneling) quantum dots, where each cell interacts with its neighbor (through Coulomb forces) to perform interconnect or logic functions [8]. In addition to their application in computation, groups of coupled quantum dots are expected to produce molecule-like electronic states that may show unique optical properties. While some attempts have been made at spatial ordering of quantum dots using preferential nucleation at special sites, e.g., lithographically etched ridges and pits or naturally formed ledges [10], techniques for the fabrication of assemblies of coupled dots has remained a major challenge.

We report on the self-assembled formation of closely spaced SiGe quantum dots ("quantum-dot molecules") by heterogeneous nucleation of defect-free islands near ~100 nm scale pits. An intriguing microstructure consisting of "cells" of coherent islands is observed to form along the four edges of square pits. The pits themselves are created by direct epitaxial growth on Si(100) surfaces and involve controlled Si and C depositions. Fundamental aspects of nucleation, including reorientation of the pits and strain relaxation of islands, are elaborated in our study.

Experiments were performed in a Riber molecular beam epitaxy (MBE) system with base pressure $\sim 5 \times 10^{-10}$ mbar. Si(100) substrates (oriented to better than $\pm 0.5°$) were degreased and chemically cleaned prior to loading into the MBE chamber. After outgassing overnight at 200 °C, samples were heated to ~925 °C to desorb the oxide layer. A low flux of Si was deposited during the oxide desorption process to obtain a smooth surface. Sharp (2×1) reconstruction patterns, consistent with the structure of clean Si(100) surfaces, were typically observed using reflection high energy electron diffraction (RHEED). Compact electron beam sources were used to deposit Si and C, calibrated at rates of ~0.2 and 0.01 nm/min, respectively. Germanium was deposited from a calibrated pyrolitic boron nitride Knudsen source at a rate of 0.15 nm/min.

A typical experiment consisted of the following steps. After the oxide desorption process was completed, C and Si were codeposited for 2–3 min on the clean Si surface at ~925 °C. The sample was then cooled to 550 °C and a thin Si buffer layer (~12–15 nm thick) was grown. The surface showed a sharp (2×1) RHEED pattern at the completion of the buffer layer growth. The SiGe alloy (nominal composition 40% ± 10% Ge) was subsequently deposited at various temperatures between 600–700 °C until the RHEED pattern indicated 3D growth. All samples were analyzed *ex situ* using atomic force microscopy (AFM). Several samples were also analyzed by plan-view and cross-sectional transmission electron microscopy (TEM).

Figures 1(a) and 1(b) show AFM images (from two different samples) of a Si(100) surface after the deposition of ~3–4 nm of SiGe at 650 °C. An intriguing microstructure consisting of cells of closely spaced (2–5 nm apart) SiGe islands are seen to form in the vicinity of the pits. The individual islands as well as the edges of the pit are oriented along ⟨100⟩ directions. Figure 1(c) shows an AFM

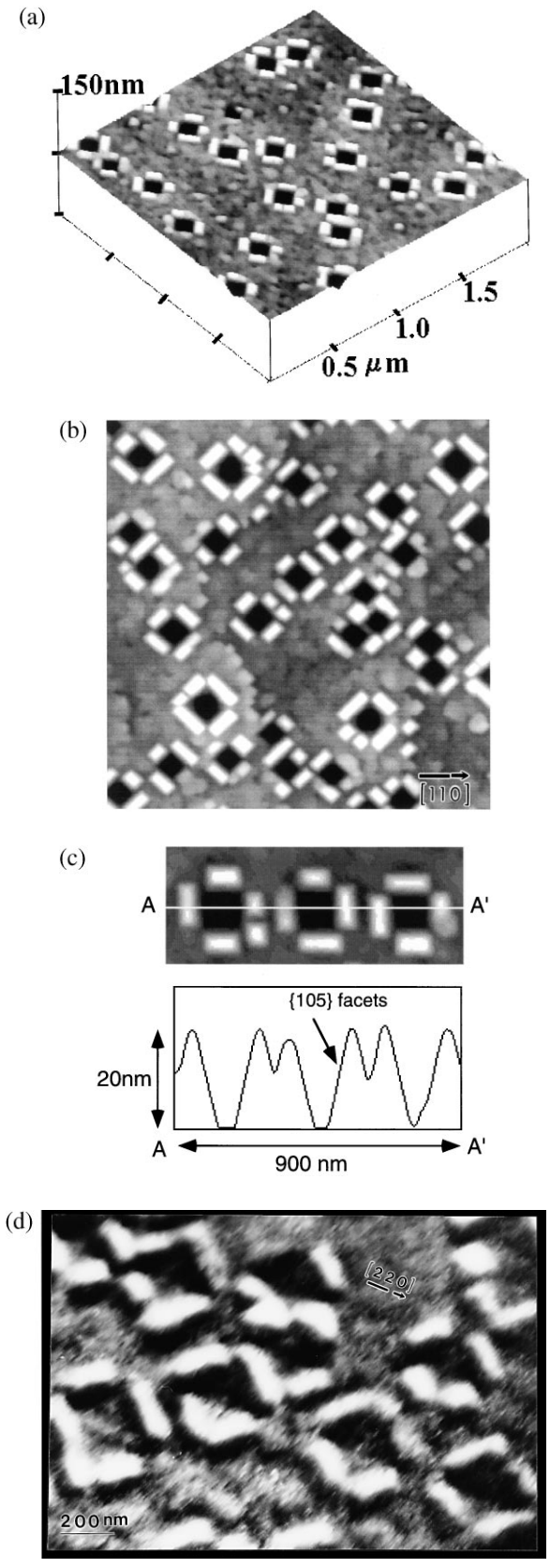

FIG. 1. Images of SiGe quantum dots at ~650 °C. (a) and (b) AFM images of the dots, 2 μm × 2 μm scan area, (c) sectional view showing the {105} facet being continuous with the pit wall, and (d) TEM dark-field image showing the strained and defect-free nature of the dots.

section analysis (along a ⟨100⟩ direction) across three adjacent cells from a region of Fig. 1(b). An interesting observation is that *each island facet is continuous with the pit wall* and makes a ~11° angle with a horizontal, consistent with {105} type faceting seen in the Si-Ge system [5,6]. Figure 1(d) is a plan-view TEM of the islands taken under two-beam dark-field conditions. It is seen that the islands are coherently strained to the substrate and are defect-free, as also confirmed by weak-beam dark-field images.

Figure 2(a) is an AFM image showing the surface morphology of a Si buffer layer grown after the initial deposition of Si and C on the original substrate. A high density of square pits is observed on the surface. The interesting point to note is that the pit edges are oriented along a ⟨110⟩ direction, unlike pits seen after the deposition of SiGe; more details on this pit "reorientation" effect are given later. A sectional analysis along the ⟨100⟩ pit diagonal is shown in Fig. 2(b). It is noted that the pit walls vary smoothly (no obvious faceting) along the growth direction and appear different from the sectional view of the SiGe covered pits seen in Fig. 1(c).

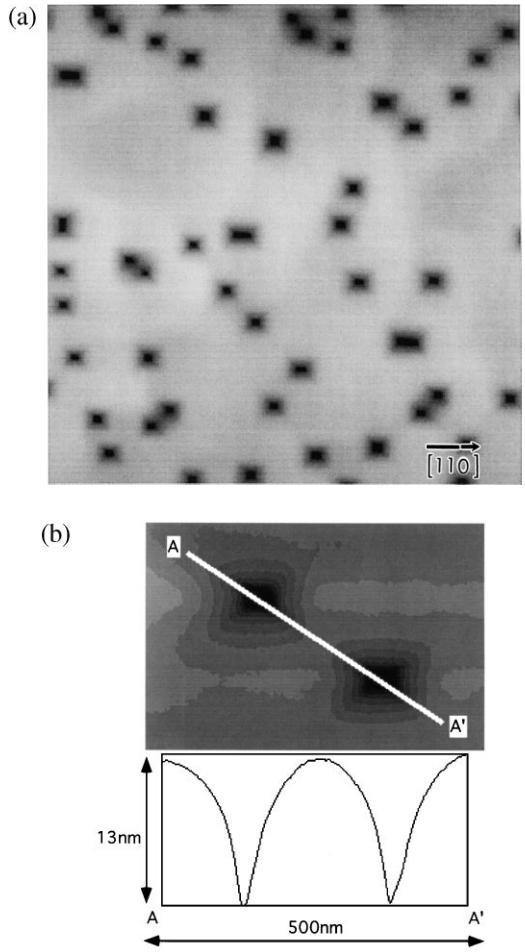

FIG. 2. Images of self-organized pits formed after controlled C and Si deposition on a Si surface. (a) AFM image, 2 μm × 2 μm scan area, and (b) sectional view showing a smoothly varying facet wall.

Figure 3(a) is an AFM image of a surface formed after ~3–4 nm growth of SiGe at 600 °C, where the growth was ceased before RHEED indicated island formation. It is noted in Fig. 3(a) that well formed, square shaped pits are uniformly distributed on the surface. The pits are again oriented along the ⟨100⟩ directions, similar to the pits seen in Fig. 1. A section analysis across two pits shown in Fig. 3(b) indicates that {105} facets have already formed along the pit walls, even before island nucleation has taken place. In addition, regions near the pits [Fig. 3(a)] show small mounds possibly associated with the initial stages of island formation.

Figure 4 shows an AFM image of SiGe deposited at 700 °C where the growth was stopped immediately after the RHEED pattern indicated island formation. The total coverage at that time was ~2 nm. Several points are noteworthy. First, the pit shape and the alignment of SiGe islands along the pits is different from that found during growth at 650 °C. Unlike the well-defined square pits with four islands each seen in Fig. 1, the microstructure in Fig. 4 shows pits that are more rounded or "octagonal" rather than square shaped and typically have six to eight islands per pit. The islands themselves are square-based prisms.

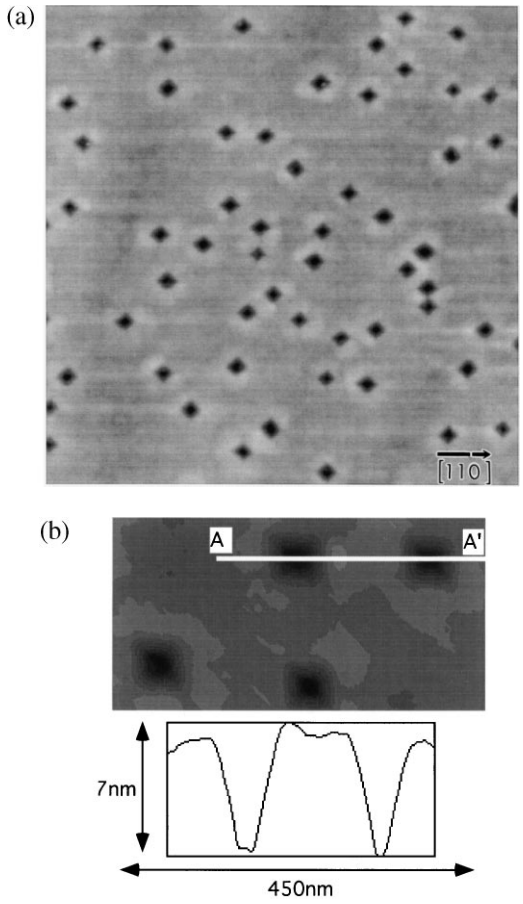

FIG. 3. Incipient stages of nucleation of SiGe dots. (a) AFM image (2 μm × 2 μm) showing well formed pits and (b) sectional view showing that the facet walls have developed into {105} type facets.

We discuss first the formation of uniform-sized (and uniform-shaped) pits on the Si(100) surface. It has been proposed previously [11] that the presence of nanometer scale coherent SiC particles (formed during *in situ* oxide desorption) on the Si surface, in conjunction with the growth of a thin Si buffer layer, can lead to the formation of pits of the surface. In the present work, we intentionally deposit a fractional monolayer of C on the Si surface immediately following oxide desorption to create a high density of SiC particles. The subsequent growth of a thin Si buffer layer naturally leads to a much higher density of surface pits. The mechanism for the formation of pits is thought to be as follows [11]. When Si is deposited on a surface with coherent SiC precipitates, the large lattice mismatch and difference in surface energy between Si and SiC cause most of the arriving Si adatoms to diffuse away from the precipitates, resulting in the formation of pits. The excess surface energy created by the pit walls is initially stabilized by the strain energy associated with heteroepitaxy of Si on SiC. With increasing buffer layer thickness, the strain energy density decreases, and the pit gradually fills in. In the present experiment, however, we are interested in the growth of a thin buffer layer to stabilize the pits. In principle, the pit dimensions can be controlled by varying the buffer layer thickness.

The preferential nucleation of SiGe islands along the four edges of the pits is intriguing from several perspectives. First, strained islands nucleating in close proximity to each other would normally be considered unusual since the local elastic strain energy increases. Nonetheless, the presence of a pit obviously influences the nucleation behavior to allow for the formation of quantum-dot molecules. Second, ideas based on classical nucleation would predict that the pit corners would be the preferred sites for nucleation [12] rather than pit edges, as observed here. How do we explain the observed nucleation pattern?

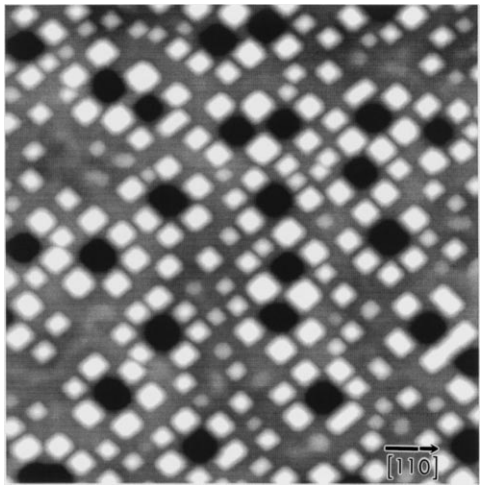

FIG. 4. AFM imaging (2 μm × 2 μm) of SiGe island nucleation at 700 °C. Note that the pits are more octagonal rather than square shaped, and that there are typically six to eight islands per pit.

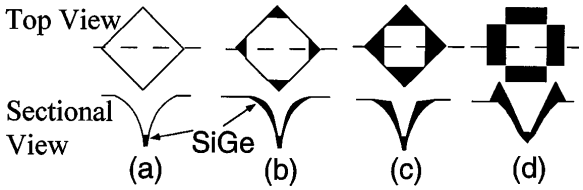

FIG. 5. Schematic depiction (top and sectional view) of the microstructural evolution of the surface during SiGe deposition. (a) Pits on the Si(100) surface and nucleation of SiGe at bottom of pit; (b) and (c) initial stages of SiGe growth and the pit "reorientation" effect; and (d) island formation and final surface morphology.

Finally, we also need to explain why the pit orientations appear different on the Si surface compared to that on a SiGe film.

The following model, described in the schematic of Fig. 5, possibly explains our observations. During the initial stages of SiGe deposition the adatoms are likely to attach near the bottom of the pit, as expected from classical nucleation [12], as shown in Fig. 5(a). Surface energy effects are typically more important than strain energy effects at initial stages of nucleation. The next stage, i.e., growth, may, however, be dominated by strain energy relaxation. Consequently, the SiGe adatoms attach preferentially at the corners of the pits, as shown schematically in Fig. 5(b). There is experimental evidence for this behavior from previous work on Ge/Si(110) [11]. Continued growth leads to filling up of the pit corners causing an apparent shape change, first to an octagonal shape, Fig. 5(b), followed by a square shape with its edges along the $\langle 100 \rangle$ directions, as shown in Fig. 5(c). By this time the walls of the pits have stabilized as {105} facets. Continued SiGe deposition leads to the formation of 3D islands whose {105} facets are simply a continuation of the pit wall. Such a scenario is depicted in Fig. 5(d) and leads to the morphology observed in Fig. 1. The microstructural features proposed in the schematic model (Fig. 5) can be correlated to our experimental observations. For example, the formation of the {105} facets before 3D island nucleation, proposed in Fig. 5(c), is evident in Fig. 3. The octagonal pit shape, depicted in Fig. 5(b) as an earlier stage of the pit-reorientation effect, can also be explained with reference to Fig. 4. Since islanding occurs earlier at 700 °C (compared to that at 650 °C), the total SiGe coverage in Fig. 4 is almost half of that in Fig. 1. Therefore, the octagonal or rounded pit shape is consistent with an earlier stage of growth.

Nucleation of islands near pits have been observed previously in conjunction with relaxation of a strained planar SiGe film activated by annealing [6]. In that case, it was proposed that islands and pits nucleate "cooperatively" due to strain relaxation obtained from the elastic interaction between pits and islands [6]. In our experiments, the {105} facet of the pit wall grows into the island facet and reduces the number of edges created by nucleation along a pit edge compared to nucleation on a flat surface. The strain energy relaxation due to the reduced number of edges may be important since the edges of the islands tend to have a large tensile stress [4,13].

Finally, we comment on another microstructural feature of interest. The growth of thicker SiGe films (beyond the stage of island formation near pits) leads to island nucleation on the flat regions away from the pits, rather than continued growth of the islands within the cluster.

In summary, we describe the fabrication of clusters of self-assembled dots (quantum-dot molecules) using a direct epitaxial growth approach. These structures may be potentially useful for devices such as the quantum-cellular automata and may possess novel electronic and optical properties.

We thank Professor Greg Snider for suggesting the term "quantum-dot molecule." We acknowledge valuable discussions with Professor T. H. Courtney, Professor J. K. Lee, and Professor D. J. Swenson, and thank Joe McLaughlin for technical help. Financial support from NSF-DMR (9624456), NSF-ECS (9707800), and a DARPA-ULTRA Nanoelectronics grant through AFOSR (F-49620-96-1-0313) are gratefully acknowledged.

*Electronic address: mohan@mtu.edu

[1] A. P. Alivisatos, Science **271**, 933 (1996), and references therein.
[2] D. Leonard, M. Krishnamurthy, C. M. Reaves, S. P. DenBaars, and P. M. Petroff, Appl. Phys. Lett. **63**, 3203 (1993); J. M. Moison *et al.*, Appl. Phys. Lett. **64**, 196 (1994).
[3] D. J. Eaglesham and M. Cerullo, Phys. Rev. Lett. **64**, 1943 (1990).
[4] S. Guha, A. Madhukar, and K. C. Rajkumar, Appl. Phys. Lett. **57**, 2110 (1990).
[5] Y-W. Mo *et al.*, Phys. Rev. Lett. **65**, 1020 (1990).
[6] D. E. Jesson *et al.*, Phys. Rev. Lett. **77**, 1330 (1996); also see D. E. Jesson, K. M. Chen, and S. J. Pennycook, Mater. Res. Bull. **21**, 31 (1996).
[7] M. Krishnamurthy, J. S. Drucker, and J. A. Venables, J. Appl. Phys. **69**, 6461 (1991).
[8] C. S. Lent *et al.*, Nanotechnology **4**, 49 (1993).
[9] A. O. Orlov *et al.*, Science **277**, 928 (1997).
[10] J. R. Heath *et al.*, J. Phys. Chem. **100**, 3144 (1996); M. Krishnamurthy *et al.*, Appl. Phys. Lett. **70**, 50 (1997); T. I. Kamins and R. S. Williams, Appl. Phys. Lett. **71**, 1201 (1997).
[11] J. D. Weil, X. Deng, and M. Krishnamurthy, J. Appl. Phys. **83**, 212 (1998); J. D. Weil, M.S. thesis, Michigan Technological University, 1997.
[12] See, for example, D. A. Porter and K. E. Easterling, *Phase Transformations in Metals and Alloys* (Van Nostrand Reinhold, Berkshire, 1981); H. I. Aaronson, J. K. Lee, and K. C. Russell, in *Precipitation Processes in Solids*, edited by K. C. Russell and H. I. Aaronson (The Metallurgical Society, Warrendale, 1978).
[13] J. K. Lee, in *Dynamics of Crystal Surfaces and Interfaces*, edited by P. M. Duxbury and T. J. Pence (Plenum Press, New York, 1997).